Electronic Supplementary Material (ESI) for Journal of Materials Chemistry A

Supporting Information

A Large-Area Smooth Graphene Film on TiO_2 nanotubes array by one-step electrochemical process

Jiangjun Xian, Danzhen Li, Jing Chen, Xiaofang Li, Miao He, Yu Shao, Linhui Yu, and Jialin Fang*

Research Institute of Photocatalysis, State Key Laboratory of Photocatalysis on Energy and Environment, Fuzhou University, Fuzhou 350002, P. R. China.
Corresponding author Tel & Fax: (+86)591-83779256, E-mail: dzli@fzu.edu.cn.

Table of contents

1. Experimental and instrumentation details

1.1 Preparation of s-TNT electrodes and TNP film coated electrodes.

The highly-ordered s-TNT electrodes were prepared by electrochemically anodizing Ti foil (2 cm × 5 cm in size, 100 μm thick, 99.5% purity, purchased from commercial market) in a two-electrode electrochemical cell with a Ti foil as working electrode and a graphite foil as counter electrode at room temperature. Before anodization, all Ti foils were orderly degreased in acetone, ethanol and distilled water for 15min by ultrasonication, respectively, and finally dried in air prior to use. The cleaned Ti foil was firstly anodized in a 200 mL ethylene glycol (EG) solution containing 0.5 wt% NH_4F and 2 vol% H_2O (i.e., 4 mL of H_2O and 196 mL of EG) at 40 V for 2 h. The obtained first-anodization TNT film (f-TNT) was removed by ultrasonication as completely as possible for few minutes, leaving behind ordered footprints (as shown in Fig. S1b) on the Ti foil (f-Ti) surface. Typically, a second anodization was then performed at 30 V for 2 h in the electrolyte previously used for first anodization, and then the highly-ordered s-TNT array was obtained after rinsed carefully by deionized water. All the anodized samples were annealed at 400 ^oC in air for 2 h with heating and cooling rate of 2 ^oC/min to convert the amorphous phase to the anatase crystalline phase. Other TNP film coated electrodes, such as Ti-TNP and ITO-TNP were prepared by a sol-gel dip-coating method. Typically, a Ti foil immersing in 50 mL TiO_2 colloid solution (about 32 mg/mL) was pulled up by a tension membrane machine at the rate of 1200 mm/h, the film was dried naturally in air. Then it was immersed in TiO_2 colloid and pulled up again. This coating action was repeated for 10 cycles. The obtained electrodes were annealed under the same conditions as TNT.

1.2 Fabrication of GR film on TNT electrodes and on other electrode materials.

The large-area fabrication of smooth GR film on s-TNT electrode was carried out by a direct current stabilized-voltage electrochemical reduction process. In the same two-electrode electrochemical cell as the anodization process, but conversely to which the working electrode of s-TNT was the cathode linked to negative wire of potentiostat, while the counter electrode of graphite foil was the anode linked to positive wire of potentiostat. The GO solution was prepared from natural flake graphite (purchased from commercial market) by a modified Hummers method,

the concentration of GO was tuned by using distilled water, and then it was exfoliated completely by ultrasonication for 10 min as the electrolyte of reduction process. Typically, the s-TNT electrode (cut into 1 cm×5 cm in size) was immersed in 50 mL exfoliated GO solution of 1 mg/mL concentration. The GR film was deposited on the surface of s-TNT at 20 V for 30 min, then the achieved s-TNT-GR composite film electrode was rinsed softly with deionized water, and dried naturally in air prior to characterization at last. Preparation of GR film on other electrode material was the same process as that on s-TNT, just to use the chosen working electrode to replace the s-TNT electrode.

1.3 Characterizations.

The FSEM images of the samples were examined using a Nova NanoSEM 230 (FEI Corp.) instrument operated at 20 kV. The AFM images of the samples were examined using a CSPM5000 (Beijing Benyuan Nanometer Instrument Co., Ltd.) instrument. The zeta potentials of GO solution with different electrochemical reaction times were determined by dynamic light scattering analysis (Zeta sizer 3000HSA) at a room temperature of 25 ^{o}C. The XPS mesurements were conducted on an ESCALAB 250 photoelectron spectrometer (Thermo Fisher Scientific) at 2.4×10^{-10} mbar using a monochromatic Al Kα X-ray beam (1486.6 eV). The binding energy (BE) of all elements was calibrated to the carbon BE of 284.5 eV. The Diffuse reflection-Fourier transform infrared (DR-FTIR) spectra were determined by using a Nicolet NEXUS 670 infrared spectrometer equipped with a diffuse reflection attachment with scanning 64 times in the range from 4000 - 500 cm^{-1}. Raman spectra were recorded at room temperature using a confocal microscopy-Raman spectrometer (Renishaw InVia) in the backscattering geometry with a 785 nm diode laser as an excitation source. The XRD patterns were recorded using a Bruker D8 Advance X-ray diffractometer equipped with a film attachment under Ni-filtered Cu Kα radiation. The accelerating voltage and the applied current were 40 kV and 40 mA, respectively. Measurements were carried out in 2θ range from 10° to 80° at the scan rate of 0.02°/s. The UV-Visible diffuse reflectance spectra (DRS) were performed on a Varian Cary 500 spectrometer with an integrating sphere attachment ranging from 200 to 800 nm. And $BaSO_4$ was used as a reference sample in DRS measurements.

1.4 Electrochemical measurements.

The in-situ oxidation reduction potential (ORP) and conductivity (Cond) of GO solution were monitored in the electrochemical reduction process of different duration times. An ORION 5-STAR Plus Meter (Thermo Fisher Scientific Inc.) connected to a computer and equipped with an ORP electrode (ORION 9678 BNWP) and a Cond cell (ORION 013605MD) was used, which were immersed in the GO solution. When the Meter began to run, the values of ORP and Cond were recorded automatically in the computer. Before the reduction voltage was power on, the ORP and Cond of GO solution were detected simultaneously for 2 min to make the stability of measurement. After the reduction voltage was power off, the measurement was still continued for 2 min.

1.5 Photocurrent measurements.

The photocurrent measurement was performed on an electrochemical workstation (CHI 660D Instrument) in a standard three-electrode system using the as-prepared sample foils as the working electrodes (cut into 1 cm × 5 cm in size) with a light area of 0.5 cm × 0.5 cm = 0.25 cm^2, a Pt wire as the counter electrode, and a Ag/AgCl (saturated in KCl) as the reference electrode. The light source was a xenon arc lamp irradiation with a filter cutting off infrared light (marked as UV-Vis, 300 nm < λ < 800 nm), and 0.1 M Na_2SO_4 aqueous solution was used as electrolyte. The bias potential was set

at 0 V vs. Ag/AgCl electrode. After every 20 seconds interval, the light irradiation was on or off to observe the change of photocurrent by using a lightproof board to open or cover the light source.

1.6 Photocatalytic activity tests.

The photocatalytic activity was evaluated by degradation of 10 μM rhodamine B (RhB) solution under the same light irradiation as the photocurrent measurements. Typically, a piece of TNT-GR composite film electrode with active area about 1 cm × 3 cm = 3 cm^2 dipping into 3 mL RhB solution in a quartz cuvette, which was 30 cm far away from light source. The light intensity on the cuvette was about 66.3 mW/cm^2. Prior to irradiation, the sample foil was kept immersing into solution to adsorb RhB molecule in dark (whole reactor was covered by a lightproof box) for 1 h to ensure the establishment of the adsorption/desorption equilibrium and then turn on the light to degrade RhB. After a specific time interval (20 min for during dark and 30 min for light), the absorbance change of RhB solution in cuvette was recorded by a Varian Cary 50 Scan UV-Vis spectrophotometer. The percentage of degradation was marked as C/C_0, here C is the maximum absorption peak intensity of RhB at 554 nm, and C_0 is the maximum absorption peak intensity of the initial RhB solution. Because the whole process of photocatalytic degradation of RhB over s-TNT400 and s-TNT400-GR were the depth mineralization processes (see Fig. S13), so they can be depicted by pseudo-first-order kinetics equation: $\ln (C_o/C) = k \times t$, where k is the photocatalytic reaction apparent rate constant, t is the reaction time, C is the real maximum absorbance peak intensity of RhB at time t, C_0 in the equation is the absorbance peak intensity at 554 nm when the dark adsorption equilibrium was achieved. To describe the photocatalytic activity more reasonably, the comparison of k value between s-TNT400 and s-TNT400-GR was demonstrated by the function of $\ln (C_o/C)$ to t (as shown in Fig. 4d).

Table S1. The name list of TNT-GR samples prepared under different conditions

Sample name	Anodization time	Anodization voltage (V)	Anodization times (h)	Annealing temprature (^{o}C)	Reduction voltage (V)	Concentration of GO (mg/mL)
f-TNT-20V2h	first	20	2	—	—	—
f-TNT-20V2h-GR	first	20	2	—	20	1
f-TNT-40V2h	first	40	2	—	—	—
f-TNT400	first	30	2	400	—	—
f-TNT400-GR-1mg/mL	first	30	2	400[b]	10	1
f-TNT400-GR(folded)	first	30	2	400[b]	20	1
s-TNT-30V2h	second	30	2	—	—	—
s-TNT400	second	30	2	400	—	—
s-TNT-40V1h	second	40	1	—	—	—
s-TNT400-40V1h	second	40	1	400	—	—
s-TNT-40V1h-GR	second	40	1	—	20	1
s-TNT400-40V1h-GR	second	40	1	400[b]	20	1
s-TNT-40V1h-GR400	second	30	2	400[a]	20	1
s-TNT-GR	second	30	2	—	20	1
s-TNT-GR400	second	30	2	400[a]	20	1
s-TNT400-GR/GR(smooth)	second	30	2	400[b]	20	1
s-TNT400-GR(folded)	second	30	2	400[b]	40	1
s-TNT400-GR-1/2mg·mL^{-1}	second	30	2	400[b]	10	1/2
s-TNT-20V1h-GR(smooth)	second	20	1	—	20	1
s-TNT-30V4h-GR(folded)	second	30	4	—	20	1
s-TNT-30V1h-GR-1/2/5mg·mL^{-1}	second	30	1	—	20	1/2/5
s-TNT-30V1h-GR-10/20/30V	second	30	1	—	10/20/30	2

[a] Annealing after the deposition of GR.

[b] Annealing before the deposition of GR.

— Represent “not has this item”.

/ Represent “or”.

2. Data processing

2.1 Analysis of the growth mechanism of the electrochemically converted graphene film.

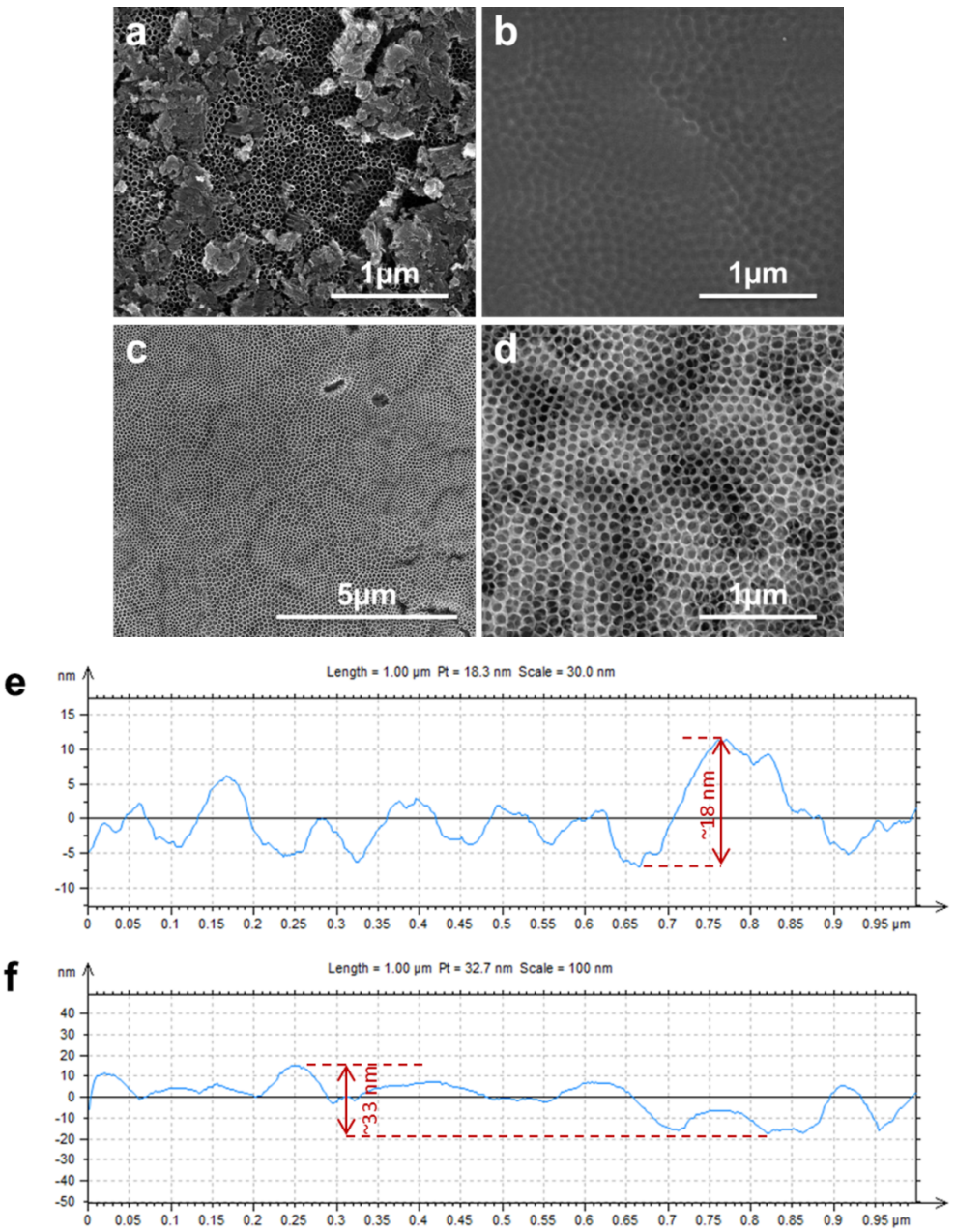

Fig. S1 (a-d) FSEM images of (a) the f-TNT-20V2h, which have a lot of impurities and sediments; (b) f-Ti (the Ti foil after removing f-TNT-40V2h film by ultrasonication), many ordered footprints of f-TNT-40V2h can be seen clearly, they will form the mesoporous layer in the second anodization;[1] (c) s-TNT-40V1h with no annealing in a low magnification, which have a very clear surface in a large area; (d) s-TNT400-40V1h (s-TNT-40V1h annealed at 400 ^{o}C in air), the mesoporous layer on its top is stable during the annealing process, which ensure that the GR grew on the annealed s-TNT is still smooth. (e, f) The typical average surface height of (e) s-TNT and (f) s-TNT-GR by AFM measurement. The former is about 18/2 = 9 nm, the latter is about 33/2 = 16.5 nm, thus it can be deduced that the typical average thickness of GR film on s-TNT is ~ 7.5 nm with 13 layers according to interlayer distance of ~ 0.6 nm.[2]

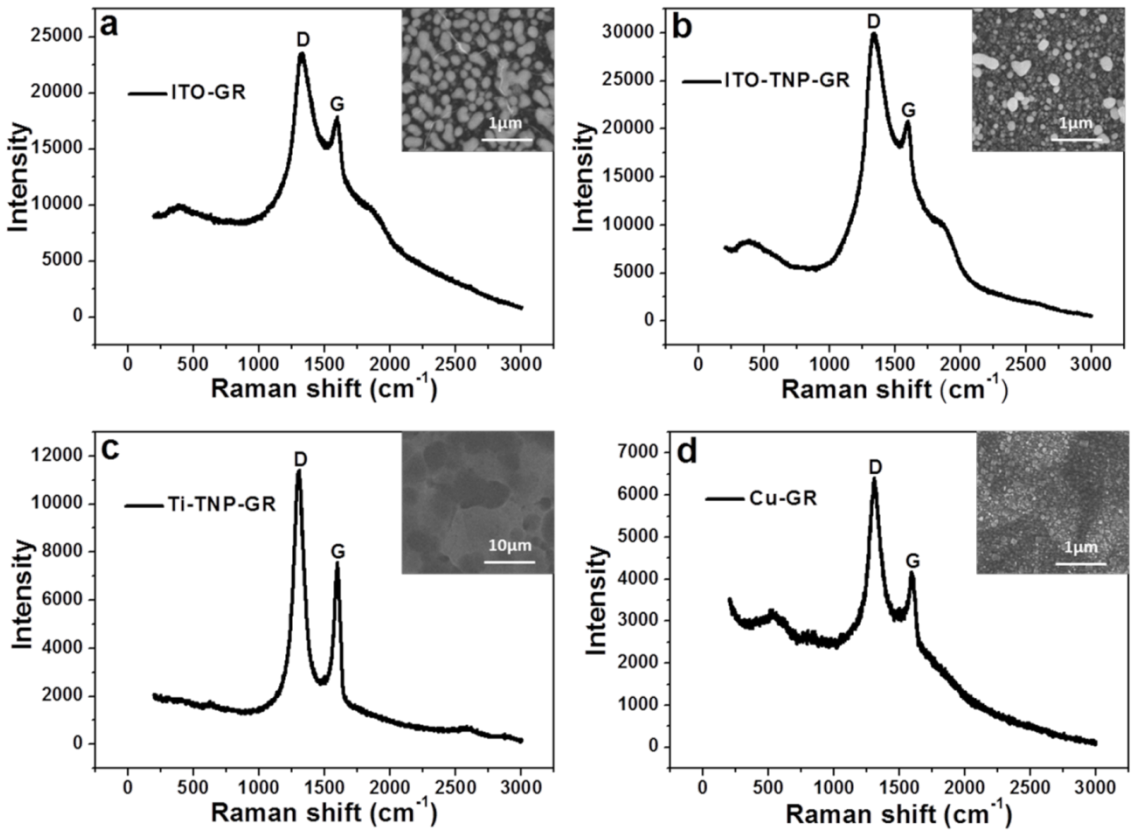

Fig. S2 The Raman spectra and FSEM images of GR film deposited on different electrode materials by the electrochemical method. The Raman spectra and relevant FSEM images of GR film deposited on (a) pure ITO, (b) ITO-TNP [TiO_2 nanoparticles (TNP) film coated ITO with no annealing], (c) Ti-TNP (TNP film coated Ti foil with no annealing) and (d) pure Cu foil electrodes. This figure shows that the GR films deposited on various electrode materials by the electrochemical method all have relatively good Raman characteristic peaks and can be seen clearly in FSEM images, indicating that the electrochemical method can be used on various substrate electrodes. In addition, the coverage of ECG films on these electrodes is smaller than that on s-TNT electrode implying the advantages of s-TNT electrode compared to other substrate electrodes.

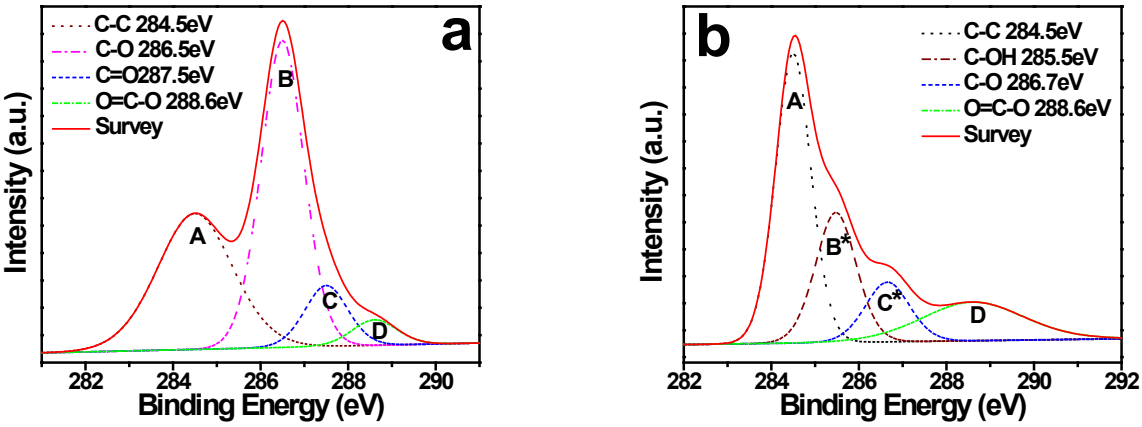

Cathode reactions:

$G\text{-}OH + e^- = G^{\bullet -} + {}^{\bullet}OH$

$G^{\bullet -} + H^+ = G\text{-}H$

$H^+ + e^- = H^{\bullet}$

$H^{\bullet} + {}^{\bullet}OH = H_2O$

$G{=}O + e^- = G\text{-}O^{\bullet -}$

$G\text{-}O^{\bullet -} + H^+ = GH\text{-}O^{\bullet}$, $H^+ + e^- = H^{\bullet}$

$GH\text{-}O^{\bullet} + H^{\bullet} = GH\text{-}OH$

$G\text{-}COOH + e^- = G\text{-}CO^{\bullet -} + {}^{\bullet}OH$

$G\text{-}CO^{\bullet -} + H^+ = G\text{-}CHO$, $H^+ + e^- = H^{\bullet}$

$H^{\bullet} + {}^{\bullet}OH = H_2O$

Anode reactions:

$G\text{-}OH = G\text{-}O^{\bullet -} + H^+$

$G\text{-}O^{\bullet -} = G{=}O + e^-$

Fig. S3 The XPS fine spectrum of C element in the samples of (a) the Ti-GO (GO solution directly dried on Ti foil) and (b) the Ti-CCG (the hydrothermal CCG sheets deposited on Ti foil by drop-coating method). The survey of Ti-GO is fitted with four peaks at A 284.5, B 286.5, C 287.4, and D 288.6 eV corresponding to C-C, C-O, C=O, and O=C-O groups, respectively. After the reduction of GO, part of the C-OH is removed, the C-O-C is reduced into C-OH, the C=O is reduced into C-OH or C-O-C, and little of the O=C-O can be reduced. Therefore, the peaks of B and C in the GO move to the lower binding energy, corresponding to the peaks of B* and C* in the CCG and the ECG (Fig. 2b in the manuscript) films. Quantitative analysis of the atom ratio of C/O in the samples are listed in Table S2, on the basis of the peak area in the XPS measurements. This figure clearly demonstrates the decrease of the oxidized groups and the reduction of GO into GR.

In addition, the corresponding detailed reactions about electrochemical reduction of GO with different oxidation groups are deduced and shown above. Wherein, G-OH, G=O, G-COOH represent a GO unit with different oxygen groups; G-H represents a GR unit after complete reduction of a GO unit with oxygen groups, G=O represents a GO unit with a C=O group or with a C-O-C group, $G^{\bullet -}$ represents a GR unit (G-H) after loss of a hydrion, $G\text{-}O^{\bullet -}$ represents a GO unit with C-OH group (G-OH) after loss of a hydrion. From these cathode reactions, we can see that each loss of a C–OH or a C=O group needs $2H^+$ and $2e^-$, thus we can deduce the overall equations for electrochemical reduction of GO into GR.

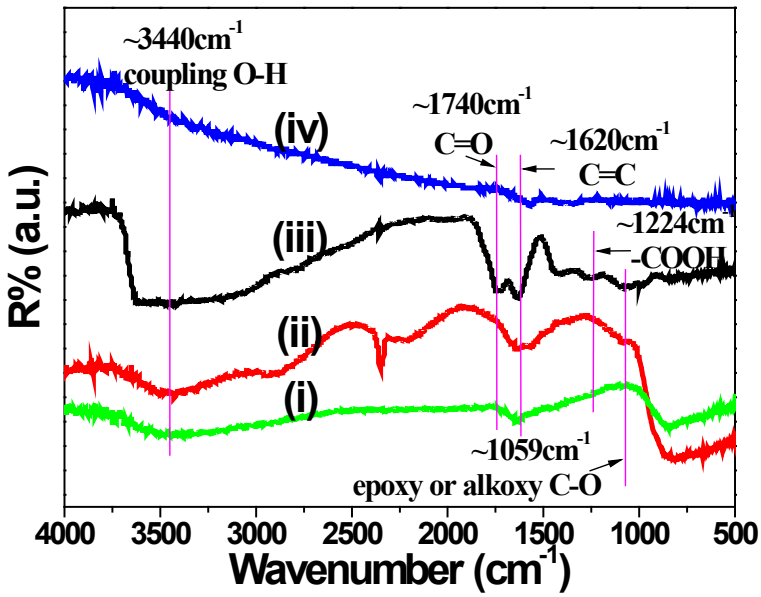

Fig. S4 The DR-FTIR spectra of the GR film deposited on different substrate materials. The DR-FTIR spectra of (i) the Ti-TNP400-GR (GR film deposited on the TNP400 film coated Ti foil), (ii) the s-TNT400-GR, (iii) the Ti-GO, and (iv) the Cu-GR (GR film deposited on the Cu foil) electrodes. Except for the Ti-GO shows strong peaks at 3440, 1740, 1620 and 1224 cm^{-1} corresponding to the coupling O-H, C=O, C=C, and –COOH oxidized groups, respectively, all other GR-based composite films prepared by the electrochemical method reveal little peaks at those positions. This figure further indicates that the oxidized groups of GO are efficiently removed, that is the GO on cathode are mostly indeed reduced into GR.

Table S2. Quantitative analysis of the atom ratio of C/O in the samples of Ti-GO, Ti-CCG, s-TNT400-GR, based on the peak area of various oxidized groups in the XPS fine spectra of the C element[3] (Fig. 2c and Fig. S3).

Sample name / Peak position (C atom type)		C atom ratio (%)			
		A (C-C)	B (C-O) / B* (C-OH)	C (C=O) / C* (C-O-C)	D (O-C=O)
GO film	Ti-GO	39.91	40.59	12.49	7.01
GR film	Ti-CCG	47.06	26.32*	11.88*	14.74
	s-TNT400-GR	52.77	14.62*	20.57*	12.04

* After the electrochemical reduction process.

For the GO film, the atom ratio of C/O is calculated as the following equation:

$$C : O = (A + B + C + D) : (B + C + 2D) \quad \text{(eq1)}$$

Thus the atom ratio of C/O in the Ti-GO is about 1.490.

For the GR film, that is that calculated as the following equation:

$$C : O = (A + B^* + C^* + D) : (B^* + 0.5C^* + 2D) \quad \text{(eq2)}$$

Therefore, the atom ratio of C/O in the Ti-CCG is about 1.620, that in the s-TNT400-GR is about 2.041. Briefly, the Ti-GO has 39.91% graphitic carbon and 60.09% oxidized carbon, while 47.06% graphitic carbon and 52.94% oxidized carbon for the Ti-CCG, 52.77% graphitic carbon and 47.23% oxidized carbon for the s-TNT400-GR, further demonstrating that the electrochemical method is more efficient than the traditional chemical process for removal of oxygen-containing groups of GO.

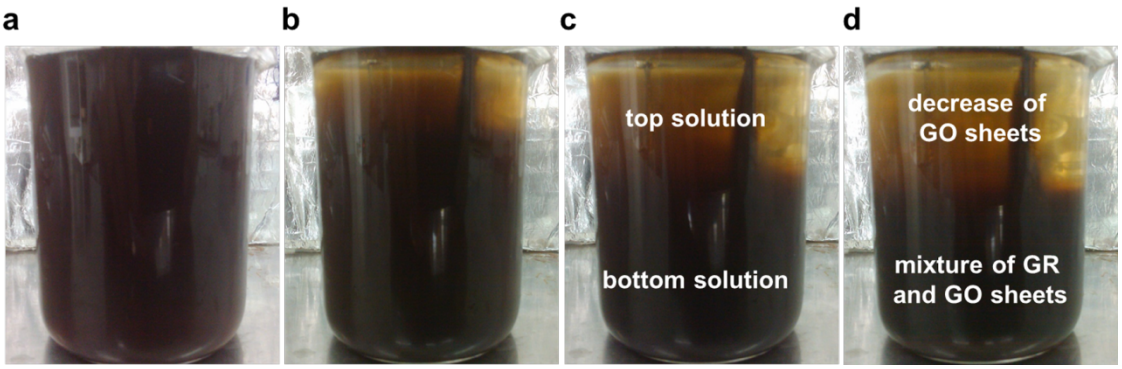

Fig. S5 The deposition process of GR sheets in the electrochemical reduction of GO solution for (a) 0 min, (b) 10 min, (c) 20 min, and (d) 30 min. With the decrease of GO and formation of GR sheets, the GO solution was separated two parts due to the deposition of partial GR sheets into the bottom solution, resulting in the mixture of GR and GO sheets. While the GR sheets adsorbed on or near by the cathode will directly deposit on the electrode surface to form the GR film.

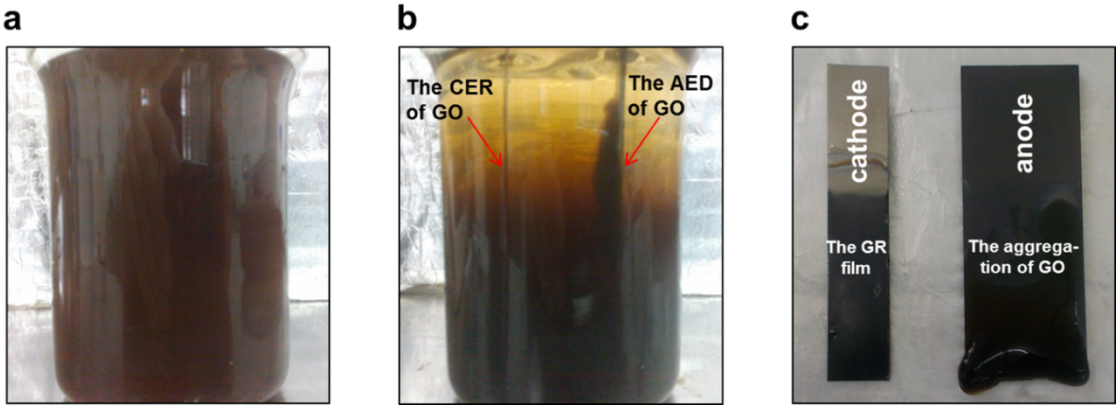

Fig. S6 The photographs of GO solution and electrodes are (a) before, (b) during and (c) after the electrochemical reduction process. Within the beginning short times, the anode electrophoretic deposition (AED) of GO sheets obviously occurred, and the cathode electrochemical reduction (CER) of GO occurred simultaneously. The CER results in the formation of GR film on the TNT surface, while the AED results in the aggregation of GO sheets on the anode graphite foil.

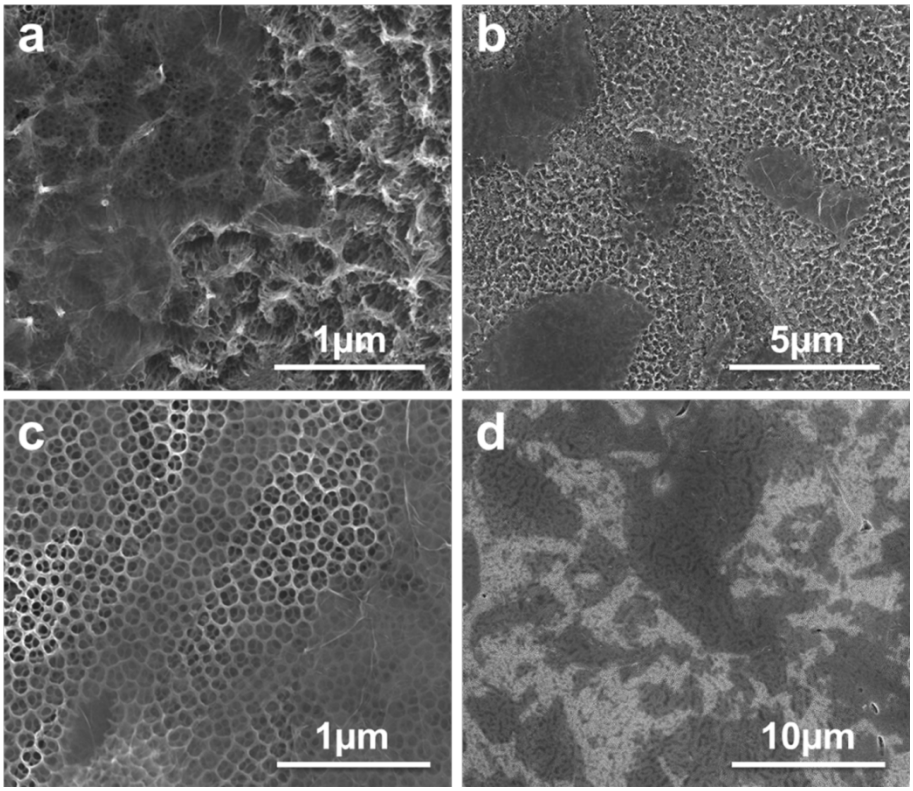

Fig. S7 The morphology comparison between f-TNT-GR and s-TNT-GR electrode. FSEM images of (a, b) the f-TNT-20V2h-GR, and (c, d) the s-TNT-30V2h-GR (abbreviated as s-TNT-GR, see the Table 1 for details) with different magnification, respectively. This figure shows that the coverage of GR on f-TNT can be improved greatly by using s-TNT.

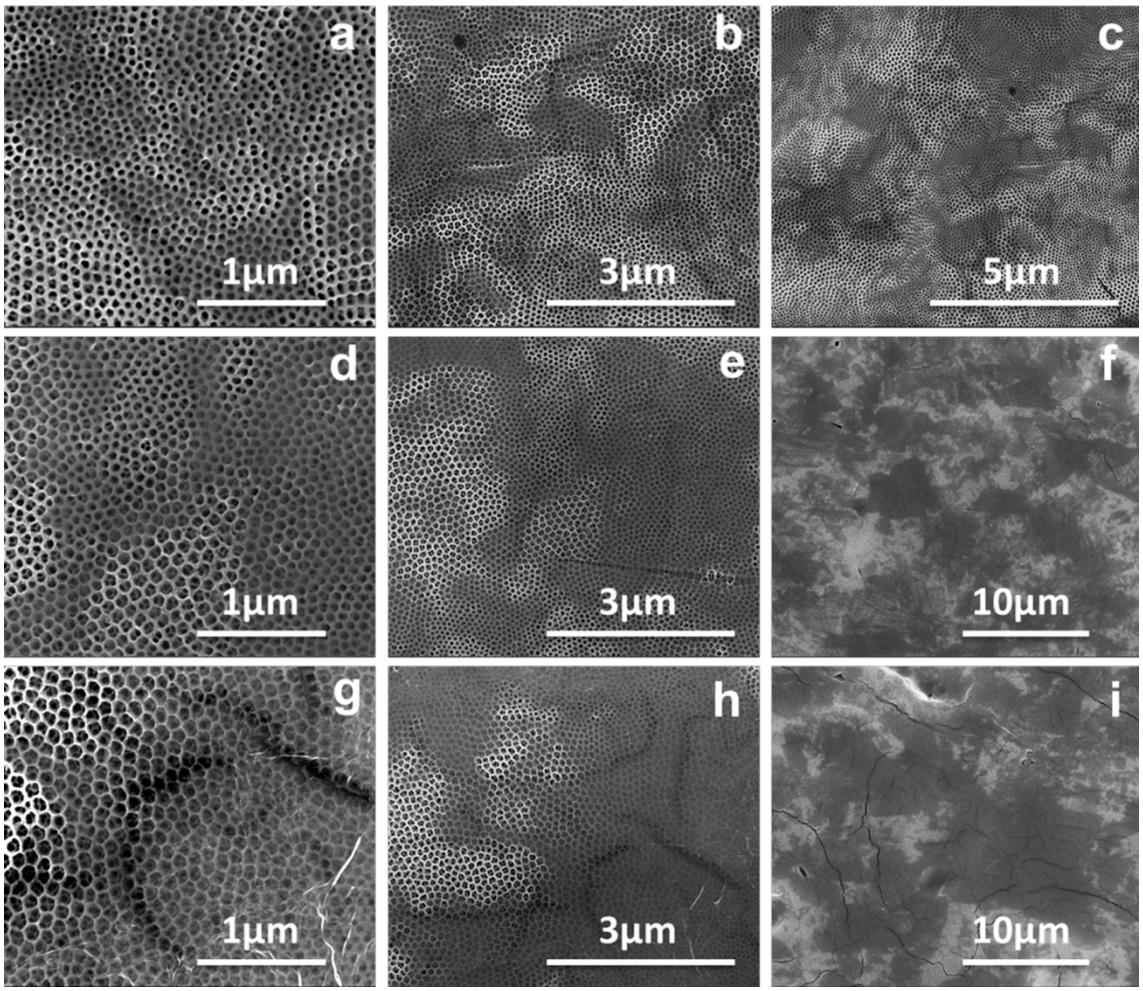

Fig. S8 The morphologies of s-TNT-30V1h-GR prepared at different reduction voltage in the same GO concentration of 2 mg/ml. FSEM images of s-TNT-30V1h-GR prepared at the reduction voltage of (a-c) 10 V, (d-f) 20 V, (g-i) 30 V with different magnification, respectively. This figure shows that the increase of reduction voltage will result in more wrinkles due to the stronger electric field force.

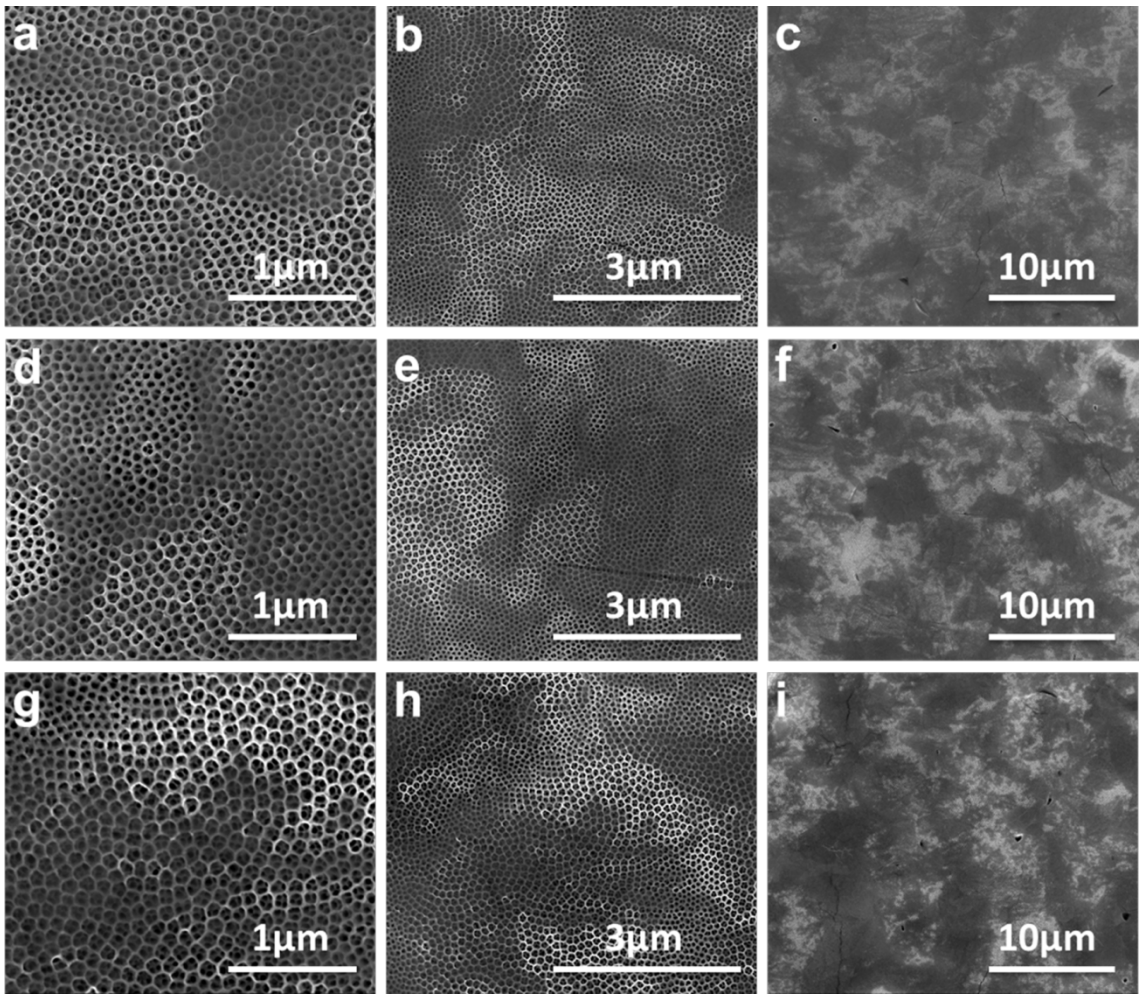

Fig. S9 The morphologies of s-TNT-30V1h-GR prepared in different GO concentration at the same reduction voltage of 20V. FSEM images of s-TNT-30V1h-GR prepared in the GO concentration of (a-c) 1 mg/mL, (d-f) 2 mg/mL, (g-i) 5 mg/mL with different magnification, respectively. This figure shows that the increase of GO concentration will enhance the coverage and thickness of GR over the electrode.

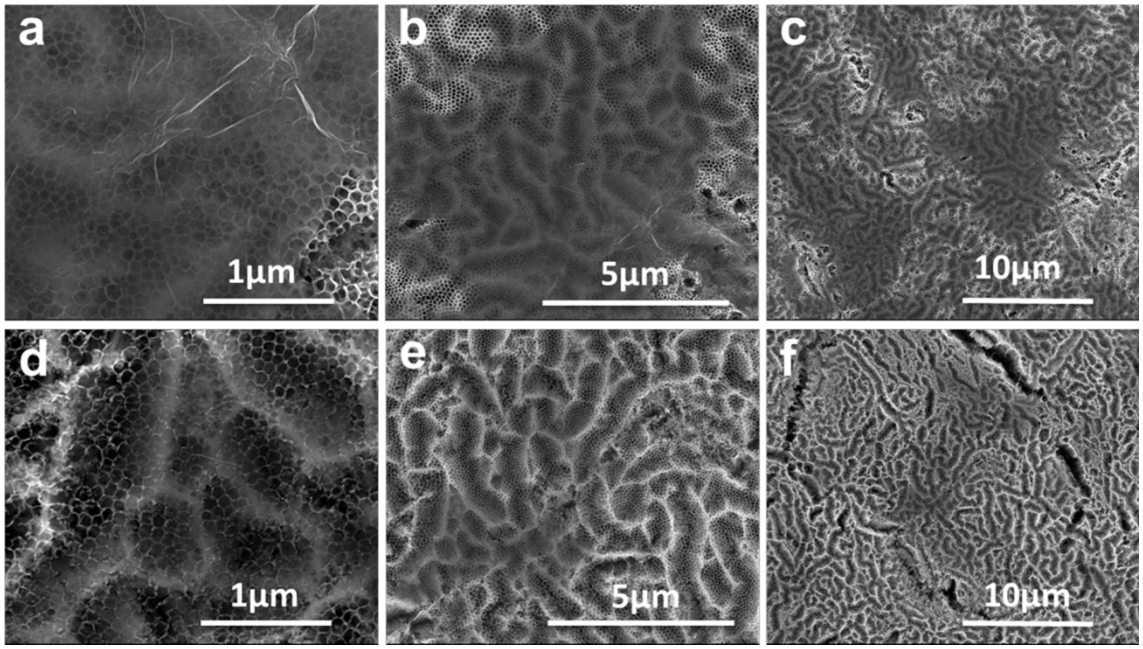

Fig. S10 The morphologies of s-TNT-40V1h-GR with different annealing treatment. FSEM images of (a-c) s-TNT400-40V1h-GR (reduction after annealing), (d-f) s-TNT-40V1h-GR400 (annealing after reduction) with different magnification, respectively. This figure shows that annealing of TNT-GR will decrease the coverage and thickness of GR film due to its intrinsic thermo nature, so we should anneal the TNT before deposition of GR or anneal the TNT-GR at a appropriate temperature.

2.2 Characterization of the electrochemically converted graphene film.

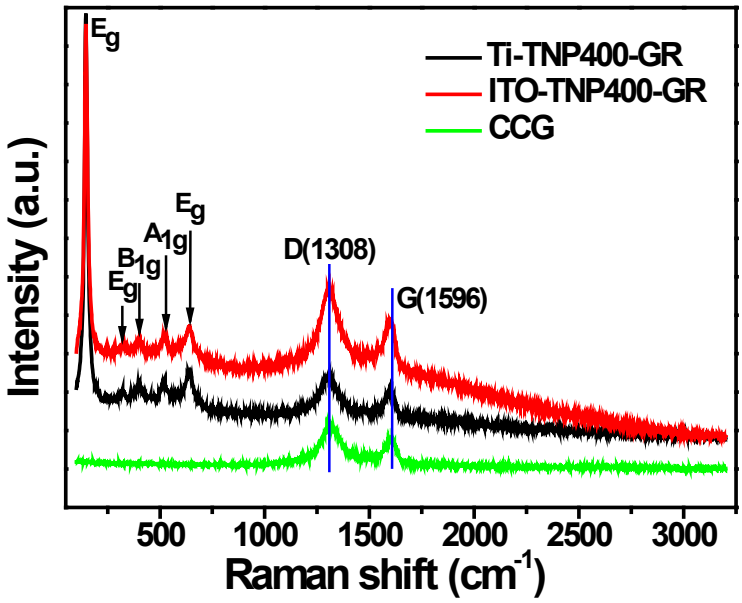

Fig. S11 The Raman spectra of GR film deposited on Ti-TNP and ITO-TNP. The characteristic Raman peaks of anatase TNP and GR are all clearly presented in the spectra. The D band and G band of GR film prepared by the electrochemical method are at the same position of CCG film. This figure indicates that the GR film can also be well deposited on TNP film with good Raman characteristic peaks by the electrochemical method.

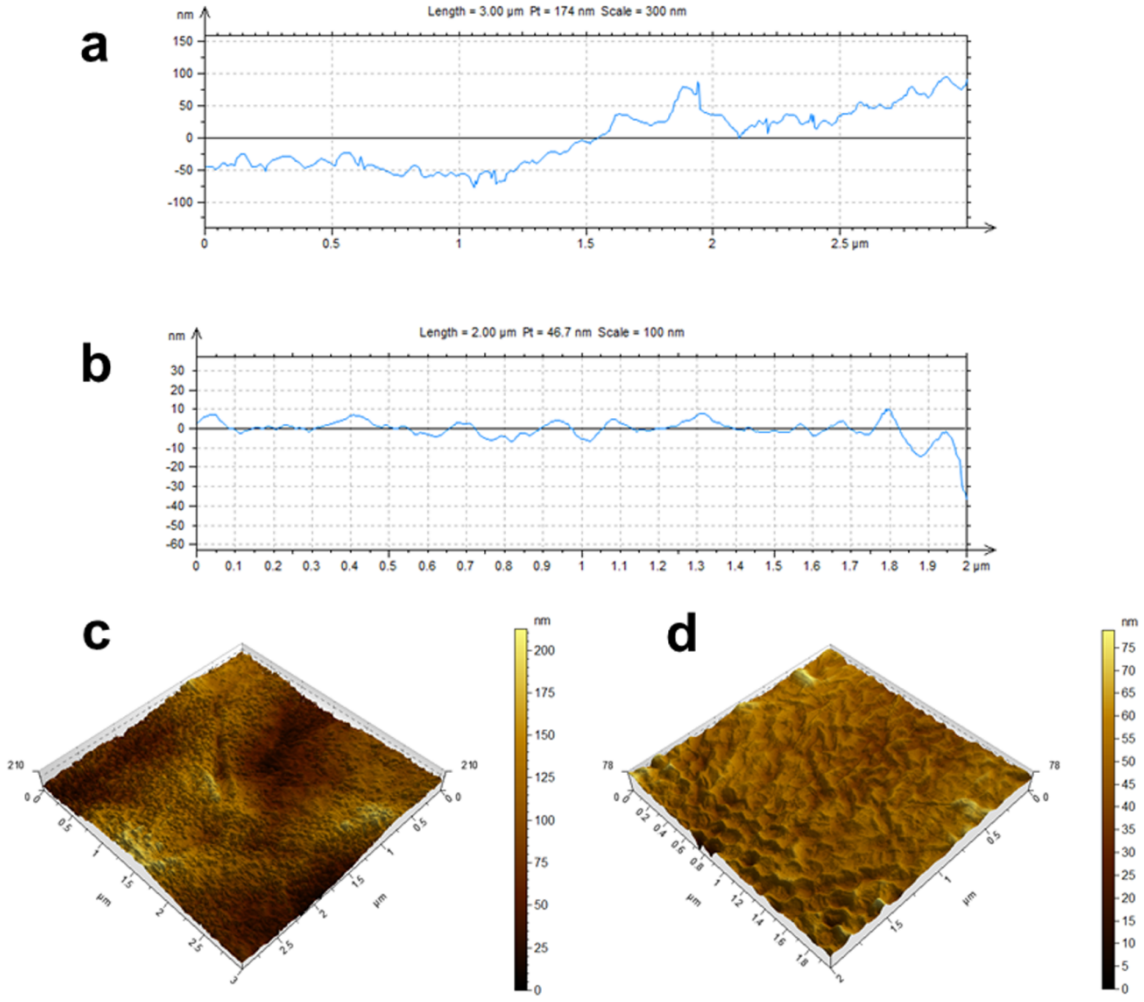

Fig. S12 (a, b) The section analysis of AFM images (Figure 3g, 3h in manuscript) along with the red line from top to bottom and (c, d) the 3D results for (a, c) f-TNT400-GR(folded) and (b, d) s-TNT400-GR(smooth), respectively. Although the whole surface height difference contains the errors caused by the porous structure of TNT substrate, the smooth GR film shows the height difference only in the range of tens nanometers, which are much smaller than the huge folds of hundreds of micrometers in usual GR films.

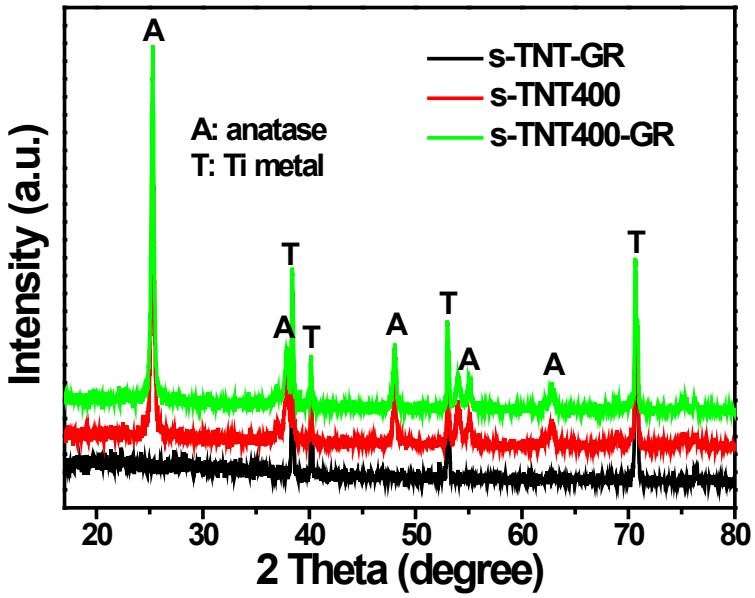

Fig. S13 The XRD patterns of s-TNT-GR with different annealing treatment. There is no obvious characteristic diffraction peak of GR in the XRD patterns, which may be ascribed to the thin thickness of GR and the close peak positions of GR and anatase TNT near the 25 degree. This figure shows that the GR film has little or no effect on intrinsic crystalline structure of the TNT electrode.

2.3 Comparison of photocatalytic properties between the composite films.

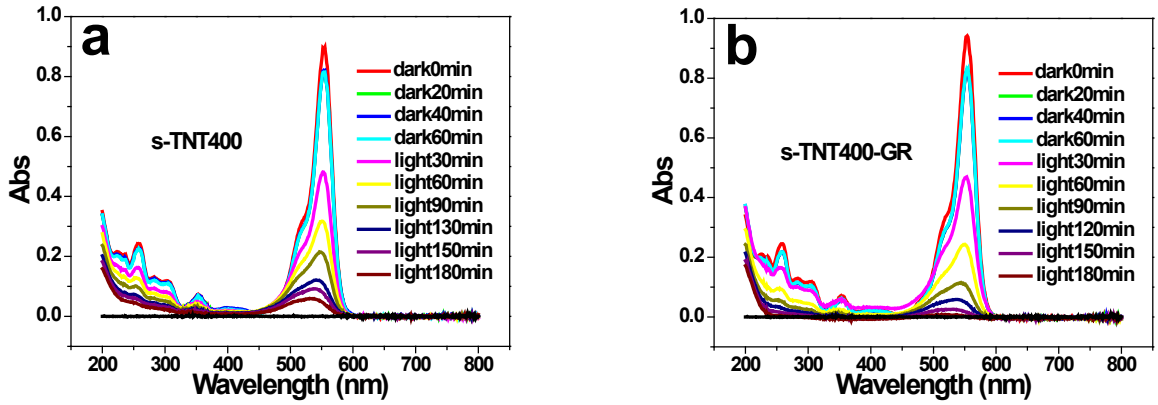

Fig. S14 The absorbance patterns of RhB solution during the whole photocatalytic degradation process by using (a) the s-TNT400 and (b) the s-TNT400-GR, respectively. For the two patterns, there's no additional peak of intermediate products except for intrinsic peaks of RhB during the whole process, suggesting that the photocatalytic degradation of 1×10^{-5} mol/L RhB over s-TNT and s-TNT-GR are depth mineralization processes, which can be approximately depicted by the pseudo-first-order kinetics model.

Table S3. The detailed data of Fig. 4d in the manuscript

Sample name	Intercept		Slope		Statistics
	Value	Standard error	Value	Standard error	R-square
P25 film	0.02789	0.05536	0.01854	5.11843E-4	0.99545
s-TNT400	-0.00832	0.0416	0.01618	3.84593E-4	0.99662
s-TNT400-GR(folded)	-0.10222	0.08594	0.01818	7.9453E-4	0.98864
f-TNT400-GR(folded)	-0.06334	0.05519	0.02075	6.0758E-4	0.99573
s-TNT400-GR(smooth)	-0.13438	0.12911	0.02598	0.00176	0.98196

Reference

[1] M. D. Ye, X. K. Xin, C. J. Lin, Z. Q. Lin, *Nano Lett*. 2011, **11**, 3214.
[2] X. Cao, D. Qi, S. Yin, J. Bu, F. Li, C. F. Goh, S. Zhang, X. Chen, *Adv. Mater*. 2013, **25**, 2957.
[3] A. Iwase, Y. H. Ng, Y. Ishiguro, A. Kudo, R. Amal, *J. Am. Chem. Soc.* 2011, **133**, 11054.